Journal of the Taiwan Institute of Chemical Engineers 42 (2011) 701–708

Contents lists available at ScienceDirect

Journal of the Taiwan Institute of Chemical Engineers

journal homepage: www.elsevier.com/locate/jtice

Key features for designing M2 proton channel anti swine flu inhibitors

Tung-Ti Chang [a,b], Mao-Feng Sun [a,c], Hsin-Yi Chen [d], Fuu-Jen Tsai [d,e], Jaung-Geng Lin [a], Calvin Yu-Chian Chen [a,d,f,g,*]

[a] Laboratory of Computational and Systems Biology, School of Chinese Medicine, China Medical University, Taichung 40402, Taiwan
[b] Department of Chinese Pediatrics, China Medical University Hospital, Taiwan
[c] Department of Acupuncture, China Medical University Hospital, Taiwan
[d] Department of Bioinformatics, Asia University, Taichung 41354, Taiwan
[e] Department of Medical Genetics, Pediatrics and Medical Research, China Medical University Hospital and College of Chinese Medicine, China Medical University, Taichung 40402, Taiwan
[f] Harvard-MIT Division of Health Sciences and Technology, 77 Massachusetts Avenue, Cambridge, MA 02139, USA
[g] Computational and Systems Biology, Massachusetts Institute of Technology, Cambridge, MA 02139, USA

ARTICLE INFO

Article history:
Received 12 August 2010
Received in revised form 24 December 2010
Accepted 11 January 2011
Available online 22 March 2011

Keywords:
H1N1
M2 proton channel
Docking
Molecular dynamics
Traditional Chinese medicine (TCM)

ABSTRACT

M2 is a crucial influenza virus proton channel that facilitates viral infection. One of the common treatments for influenza is to inhibit M2 function. However, these commercially available M2 inhibitors became less effective against new drug-resistance viral strains, such as the H1N1 influenza virus that caused 2009 flu pandemic. Therefore, it became urgent to develop more effective drugs against the new influenza strains. This study focused on identifying potential M2-inhibiting compounds from traditional Chinese medicine (TCM) using a freely accessible TCM database (http://tcm.cmu.edu.tw/) (Chen, 2011). The compounds were analyzed by computer-simulated protein–ligand interactions and then monitored through molecular dynamics (MD) simulation. The MD simulation has identified and conformationally validated five potential M2 inhibitors. Further bio-molecular experiments would be required to validate their bioactivities. In addition, the MD simulation technique provides insights to next generation of drug design.

1. Introduction

The M2 proton channel is a class of influenza membrane protein that plays an important role in the viral replication cycle. A functional M2 tetramer consist a short N-terminal, a C-terminal tail, and a transmembrane domain for transporting protons (Pinto *et al.*, 1997; Sugrue and Hay, 1991). The primary function of M2 is to facilitate proton entry to viral interior (Helenius, 1992). The acidic pH at viral interior caused by influx of protons triggers the dissociation of viral matrix protein and result the entry of viral genome (Pinto and Lamb, 2006). Hence, abolishing proton influx through M2 proton channel is an effective antiviral strategy against influenza.

The M2 inhibitor, amantadine, is a widely used influenza drug. However, amantadine-resistant viral strains, such as 2009 H1N1 pandemics, have been increasingly reported (Cheng *et al.*, 2009; Ilyushina *et al.*, 2005). Intriguingly, single amino acid change in M2, such as at residue 31N in H1N1, causes the protein to be insensitive to the drug (Squires *et al.*, 2008). Therefore, the development of novel anti-viral strategy is brought to attention (Cheng *et al.*, 2009). In this article, we investigated potential novel M2 inhibitors as well as new neuraminidase inhibitors (Du *et al.*, 2010).

We applied TCM Database@Taiwan, the world's largest traditional Chinese medicine (TCM) database (http://tcm.cmu.edu.tw/) (Chen, 2011), to investigate novel M2 inhibitor lead compounds. The TCM database has been used to screen for several novel anti-cancer or anti-inflammatory compounds (Hsieh *et al.*, 2010; Su *et al.*, 2008; Tang *et al.*, 2009). Furthermore, the diverse chemical properties of each TCM compound makes the TCM database a great source for screening novel lead compounds. Previous studies show that our research protocol has been successfully implemented for investigating new drug leads (Chen, 2007, 2008a,b,c, 2009a,b,c,d,e, 2010a,b,c; Chen and Chen, 2007; Chen *et al.*, 2008a,b, 2009a,b, 2010; Huang *et al.*, 2010a,b,c).

2. Materials and methods

2.1. Molecular docking and Lipinski's Rule of Five

The LigandFit program included in the Discovery Studio 2.5 (Accelrys Inc., San Diego, USA) was performed for ligand docking.

* Corresponding author at: Harvard-MIT Division of Health Sciences and Technology, 77 Massachusetts Avenue, Cambridge, MA 02139, USA.
Tel.: +1 617 353 7123.
E-mail addresses: ycc@mail.cmu.edu.tw, ycc929@MIT.EDU (C.-C. Chen).

1876-1070/$ – see front matter © 2011 Taiwan Institute of Chemical Engineers. Published by Elsevier B.V. All rights reserved.
doi:10.1016/j.jtice.2011.01.006

The high-resolution crystallographic structure of M2 was obtained from Protein Data Bank (PDB code: 3C9J) (Stouffer *et al.*, 2008). The amantadine present in the original M2 crystal structure was removed to obtain pure M2 structure. The amantadine was used as a control ligand. In addition, the amantadine docking region was set as the as the ligand-binding domain for the molecular docking algorithm. Compound set used for docking was obtained from TCM database (http://tcm.cmu.edu.tw/) (Chen, 2011). All compounds from the TCM database were screened and ranked by Dock Score.

Both protein and ligand structure were prepared to obtain high binding resolution. All water molecules were removed before sent for docking. Forcefield of the Chemistry at Harvard Macromolecular mechanics (CHARMm) were applied on both the TCM compounds and the amantadine before docking. Compounds having docking scores above the control (amantadine) docking score were evaluated for their drug-likeness using Lipinski's Rule of Five (Lipinski *et al.*, 2001). Five compounds with highest docking scores (top 5) were chosen for further analysis.

2.2. Molecular dynamics simulation

Molecular dynamics (MD) simulation is applied on selected protein–ligand complexes as well as the control complex using Standard Dynamics cascade of Discovery Studio 2.5. Each simulation system was pre-applied with CHARMm force field and then energy minimized with 500 and 500 steps of steepest descent and conjugate gradient minimization. Each system was heated to 310 K for 20 ps before entering 100 ps of equilibration phase. The production phase was conducted for 60 ns on a NVT ensemble at 310 K. SHAKE algorithm was applied with 2fs step size throughout the entire simulation run. The non-bonded interaction cutoff was set at 10 Å. The spherical cutoff was used to calculate long range electrostatics. A trajectory snapshot was taken every 20 ps.

3. Results and discussion

3.1. Molecular docking

To screen for TCM compounds that have similar functions as amantadine on M2, we docked the candidate molecules into the amantadine binding site. For control, we captured the amantadine 3D structure from the co-crystallized M2-amantadine structure (PDB code: 3C9J). Each ligand–M2 pair was evaluated and ranked using Dock Score. The Dock Score function was implemented in DS 2.5 to calculate binding affinity based on receptor–ligand interaction and ligand internal energy (Venkatachalam *et al.*, 2003). Top 5 compounds and the control are listed in Table 1. The compounds show significantly higher Dock Scores than amantadine, suggesting stronger binding affinities would be observed. Intriguingly, the control and all top 5 compounds do not share similar molecular structures (Fig. 1). This could imply variations of key residues that bind to each ligand.

Table 1
TCM database docking results. Shown in below are the top 5 ingredients and the control, amantadine.

Name	Dock Score
Canavanine	137.66
α-(Methylenecyclopropyl)glycine	109.388
Quinic acid	100.616
2-Hydroxy-3-(3,4-dihydroxyphenyl)propanoic acid	90.553
β-D-Fructofuranose	79.211
Amantadine	33.87

The docking conformations were investigated to further study the interactions between each ligand–M2 pair at the key residues in the binding site (Fig. 2). For all compounds, including the control, the docking conformations show close approximation to each Ser10 residue in each protein chains. Furthermore, each ligand forms hydrogen bonds (H-bonds) with at least two Ser10 residues. However, no H-bond is observed in amantadine's docking conformation, which implies lower binding affinity between amantadine and the docking site. This observation could explain the difference of the Dock Scores between top 5 compounds and the control.

3.2. Molecular dynamics simulation

To further analyze each protein–ligand conformation, molecular dynamics simulation is used to evaluate the stability after docking. Root mean squared deviation (RMSD) was used to

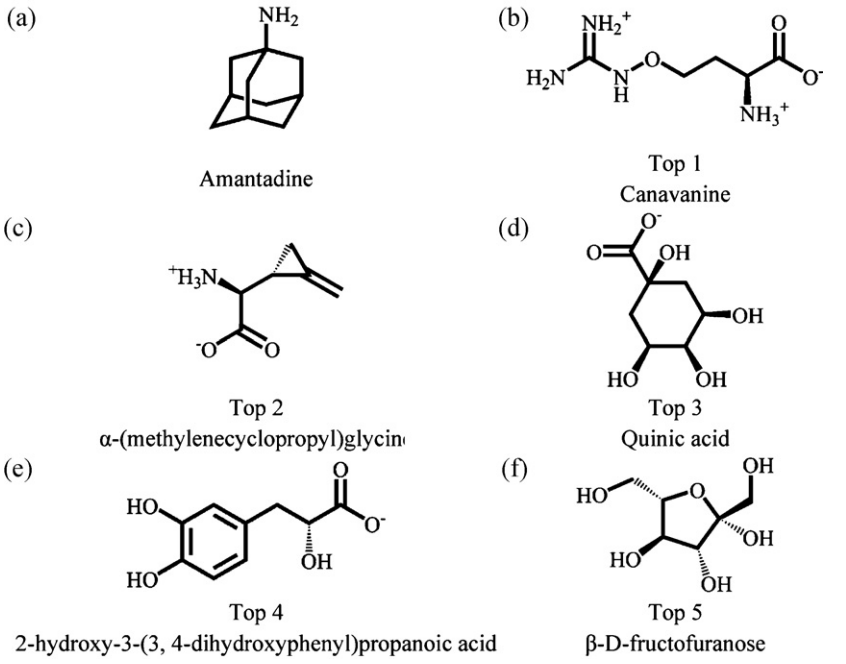

Fig. 1. The 2D structure of control amantadine and the top five compounds.

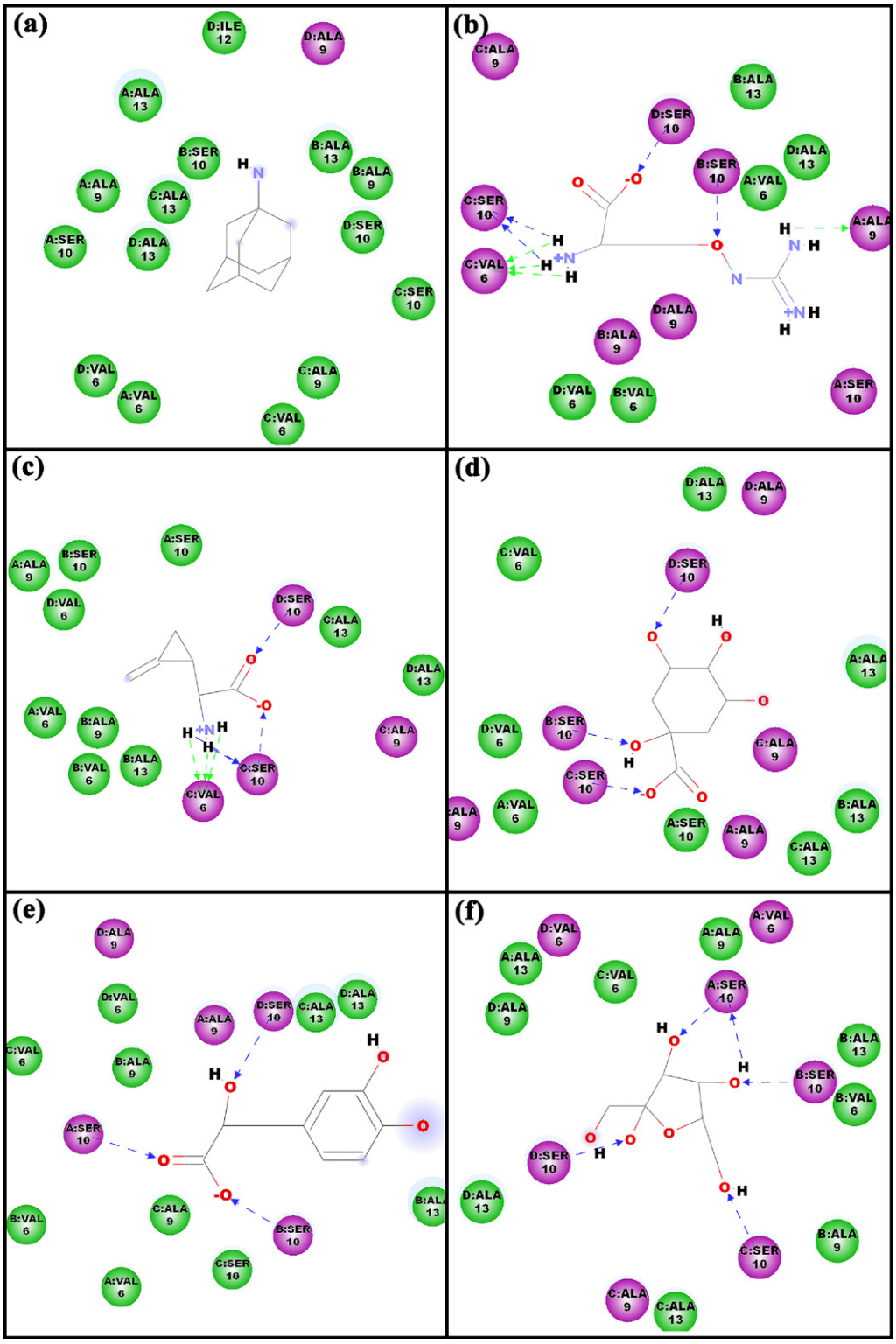

Fig. 2. The docking conformations of amantadine and top five compounds in M2 binding site.

calculate the atomic fluctuations at each time point with reference to the initial structure. MD simulation captures 50 conformational "snap shots" every nano-second for 60 ns after the initial docking conformation. RMSDs for protein–ligand complexes, as well as for ligands and for M2 proteins at Cαs separately in each complex, were calculated (Fig. 3). The RMSDs for each protein–ligand complex and for each ligand become stabilized after 50 ns. Similar trends observed between the RMSDs for complexes and the RMSDs for protein-only suggested that the fluctuations of the side chains have limited impact on RMSDs.

The canavanine–M2 complex had several stable conformations: 5–15 ns, 17–49 ns, and then stabilized after 49 ns. Based on the corresponding RMSDs, the ligand canavanine underwent a pose shift near 15 ns, and then slight shift at 49 ns, which can possibly

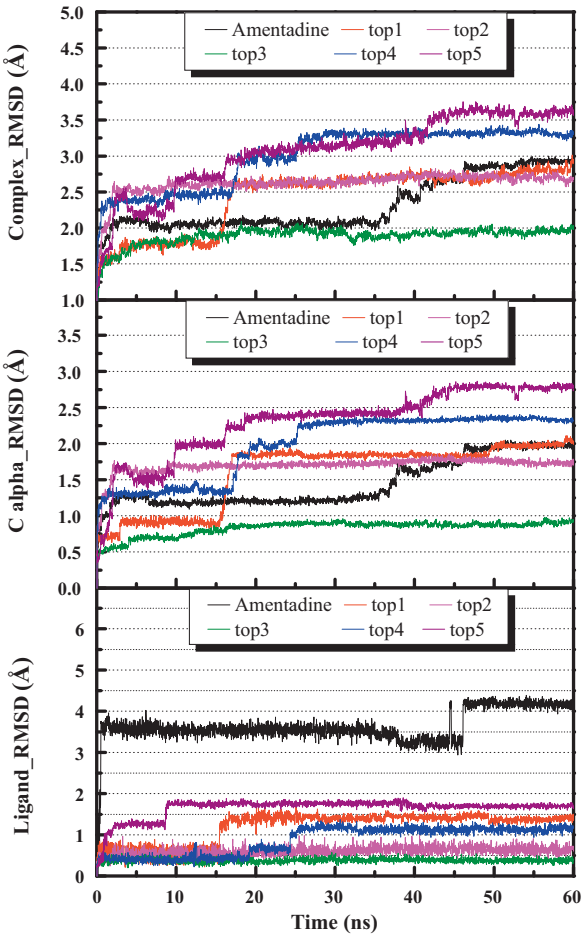

Fig. 3. Root mean square deviation of the M2–ligand complexes, C alpha and the ligands.

explain the alterations in the binding complex. Conversely, α-(methylenecyclopropyl)glycine and quinnic acid conformations stabilized after 5 ns. In addition, their corresponding RMSDs for the protein and the complex stabilized after 15 ns. All selected compound-protein complexes stabilized after 27 ns, except the least stable β-D-fructofuranose–protein complex, in which slight ligand fluctuations result steady conformational changes in M2 after 42 ns. For the control amantadine, RMSDs for the protein–ligand complex revealed a conformational change after 36 ns. The

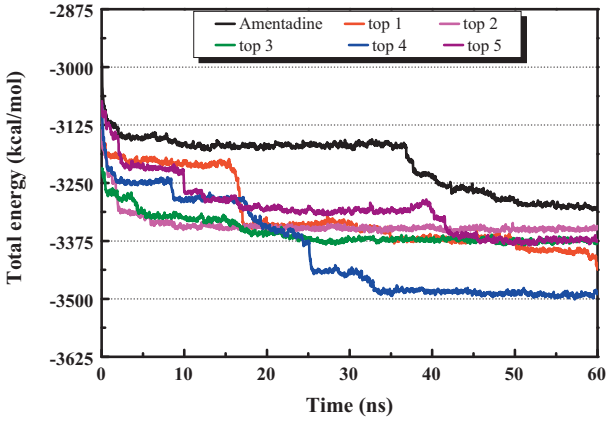

Fig. 4. Total energy of M2 complexes with amantadine and top five compounds.

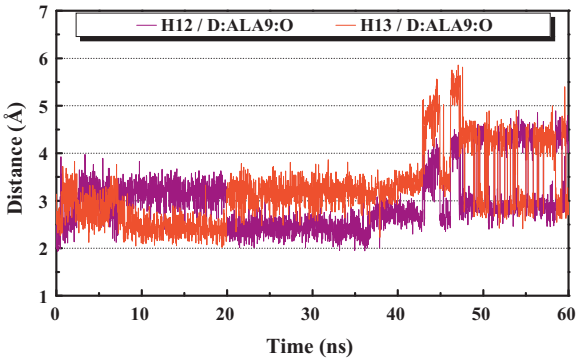

Fig. 5. Hydrogen bonds formed between amantadine and M2 residues.

conformation stabilized after amantadine underwent a post shift around 47 ns.

The observed RMSD trend for each protein–ligand complex is validated by total energy (Fig. 4). Stable total energy drops were observed for protein–ligand complex of α-(methylenecyclopropyl)glycine and quinnic acid. The multiple stable energy states for canavanine–protein complex corresponded accurately to the multiple stable conformations. Gradual declining total energy for the control amantadine after 36 ns also suggested a potential shift in the binding structure conformation.

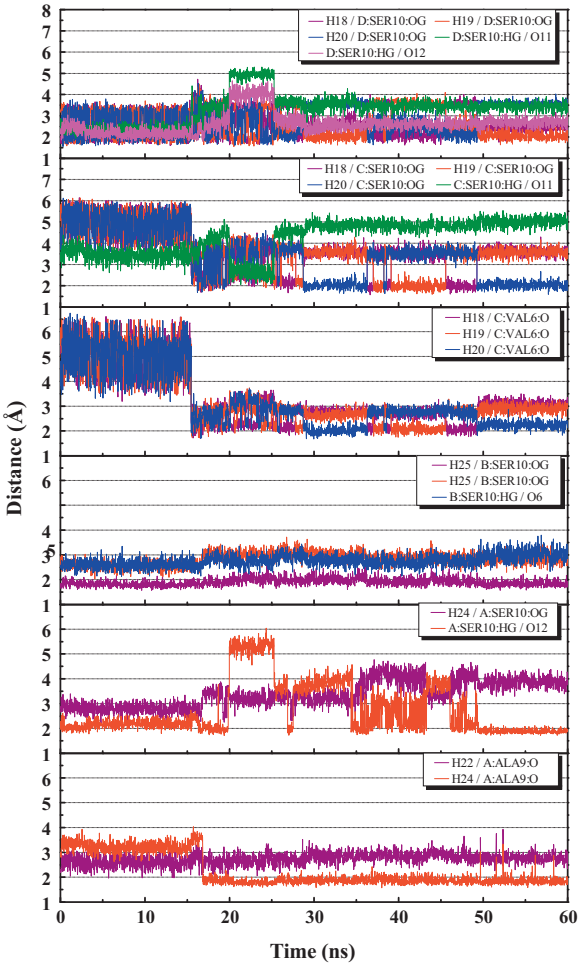

Fig. 6. Distance of hydrogen bonds formed between M2 residues and top 1 during the 60 ns molecular dynamics simulation.

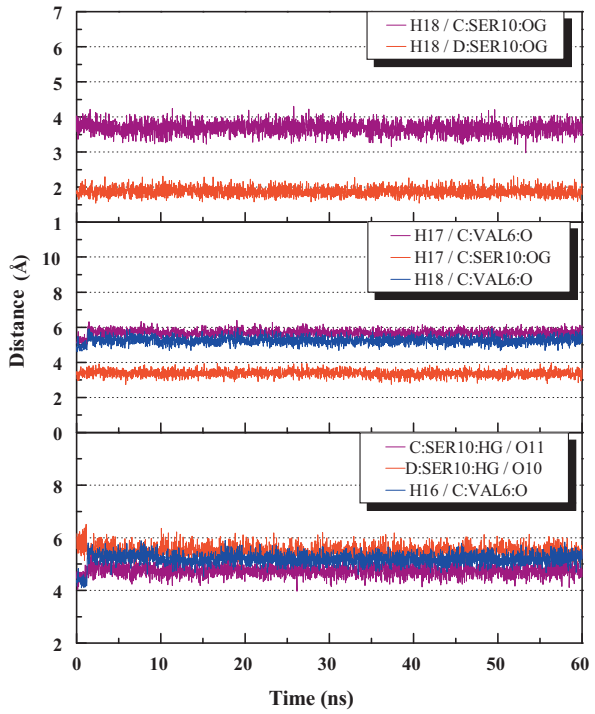

Fig. 7. Distance of hydrogen bonds formed between M2 residues and top 2 during the 60 ns molecular dynamics simulation.

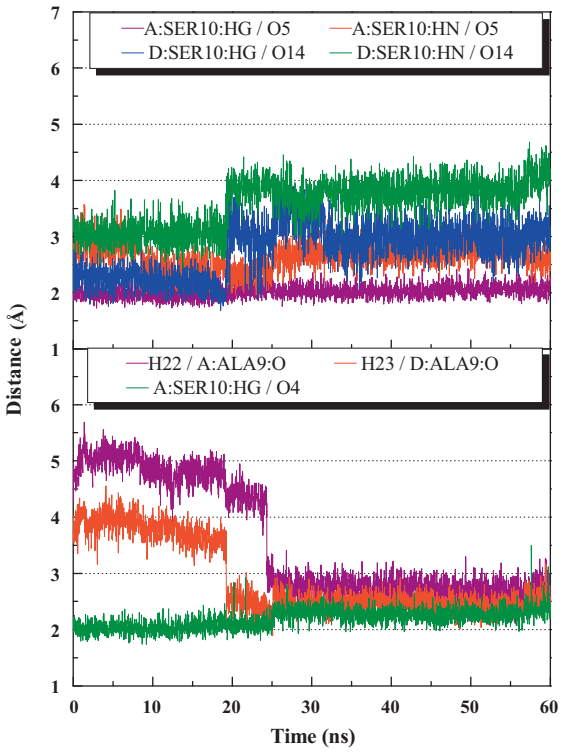

Fig. 9. Distance of hydrogen bonds formed between M2 residues and top 4 during the 60 ns molecular dynamics simulation.

The changes in RMSDs and total energy suggested fluctuations in each protein–ligand conformation. Hence, the stabilized docking conformations after MD simulation were re-investigated for the binding interactions. In particular, H-bonds, which were key players in stabilizing energetically favored ligands (Patil *et al.*, 2010), were evaluated (Table 2). Surprisingly, the NH_2 group from the control amantadine skeleton formed an H-bond with Ala9 on one of the M2 subunits at distance of 3 Å. The H-bond formed after MD simulation implied a relatively more stable protein–ligand conformation. Furthermore, the stable amantadine pose main-

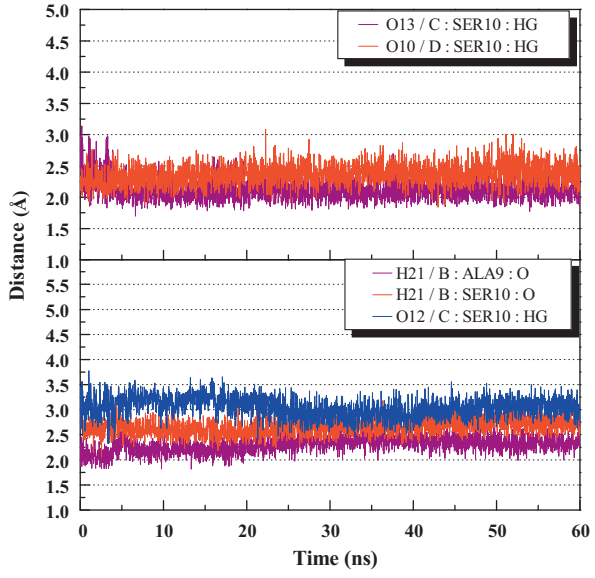

Fig. 8. Distance of hydrogen bonds formed between M2 residues and top 3 during the 60 ns molecular dynamics simulation.

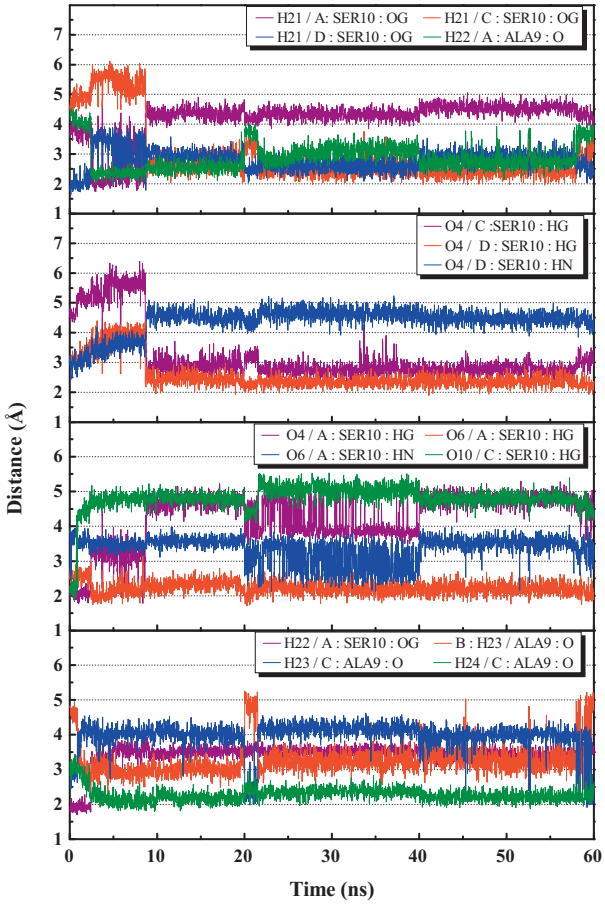

Fig. 10. Distance of hydrogen bonds formed between M2 residues and top 5 during the 60 ns molecular dynamics simulation.

Table 2
Summady of hydrogen bonds formed between amantadine, top 1 (canavanine), top 2 (alpha-(methylene-cyclopropyl) glycine), top 3 (quinic acid), top 4 (2-hydroxy-3-(3,4-dihydroxyphenyl) propanoic acid), and top 5 (β-D-fructofuranose) during the 60 ns molecular dynamics simulation.

Compound	H-bond	Max. distance	Min. distance	Ave. distance	% of occupancy
Amantadine	H12/D:ALA9:O	4.91	1.93	2.97	23.00
	H13/D:ALA9:O	5.86	2.02	3.23	15.00
Top 1	H22/A:ALA9:O	3.92	1.86	2.74	14.90
	H24/A:ALA9:O	4.03	1.58	2.25	71.74
	H24/A:SER10:OG	4.76	2.10	3.38	2.17
	A:SER10:HG/O12	6.04	1.71	2.76	62.61
	H25/B:SER10:OG	2.68	1.57	1.90	99.90
	B:SER10:HG/O6	3.72	2.03	2.83	10.03
	B:SER10:HN/O6	3.80	2.13	2.76	13.93
	H18/C:VAL6:O	6.62	1.71	3.33	20.83
	H19/C:VAL6:O	6.59	1.72	3.27	22.73
	H20/C:VAL6:O	6.74	1.68	3.16	36.25
	H18/C:SER10:OG	6.13	1.58	3.69	17.09
	H19/C:SER10:OG	6.13	1.60	3.65	18.99
	H20/C:SER10:OG	6.11	1.60	3.38	35.22
	C:SER10:HG/O11	5.54	2.06	4.24	3.20
	H18/D:SER10:OG	4.72	1.60	2.65	50.78
	H19/D:SER10:OG	4.50	1.55	2.57	60.48
	H20/D:SER10:OG	4.53	1.55	2.83	41.09
	D:SER10:HG/O11	5.30	1.94	3.31	21.09
	D:SER10:HG/O12	4.65	1.73	2.64	41.12
Top 2	H18/D:SER10:OG	2.32	1.55	1.87	100.00
Top 3	H21/B:ALA9:O	2.79	1.82	2.30	90.33
	H21/B:SER10:O	3.22	2.06	2.67	15.20
	O12/C:SER10:HG	3.78	2.33	3.05	0.23
	O13/C:SER10:HG	3.14	1.70	2.12	97.33
	O10/D:SER10:HG	3.09	1.84	2.37	80.57
Top 4	H22/A:ALA9:O	5.69	2.11	3.56	7.10
	H23/D:ALA9:O	4.55	1.89	2.89	41.15
	A:SER10:HG/O4	3.50	1.74	2.19	97.70
	A:SER10:HG/O5	2.48	1.73	2.02	99.97
	A:SER10:HN/O5	3.57	1.92	2.65	26.92
	D:SER10:HG/O14	4.09	1.69	2.79	32.12
	D:SER10:HN/O14	4.68	2.43	3.58	0.03
Top 5	H21/A:SER10:OG	5.06	1.74	4.19	6.27
	H21/C:SER10:OG	6.12	1.96	2.96	39.77
	H21/D:SER10:OG	3.92	1.63	2.79	18.10
	H22/A:ALA9:O	4.51	1.97	2.87	19.83
	H22/A:SER10:OG	4.09	1.70	3.42	4.03
	B:H23/ALA9:O	5.26	2.34	3.27	0.17
	H23/C:ALA9:O	4.63	1.91	3.97	3.60
	H24/C:ALA9:O	3.44	1.80	2.28	90.10
	O4/A:SER10:HG	5.29	1.78	4.26	4.40
	O6/A:SER10:HG	3.30	1.72	2.24	90.60
	O6/A:SER10:HN	4.03	2.13	3.36	4.57
	O10/C:SER10:HG	5.53	1.83	4.81	1.30
	O4/C:SER10:HG	6.39	2.11	3.19	3.47
	O4/D:SER10:HG	4.40	1.90	2.56	67.10
	O4/D:SER10:HN	5.23	2.43	4.39	0.03

tained each M2 subunit at close approximation. This conformation suggested the blocking of M2 proton transportation function.

Based on the calculation of potential H-bonds during the 60 ns MD simulation, Ala9 and Ser10 in each homologous M2 subunits appeared to be critical sites for H-bond formation. For the control, amantadine formed H-bonds to the nearby Ala9 residues (Fig. 5). All top 5 ligands formed at least one H-bond to the nearby Ser10 residues (Table 2 and Figs. 6–10). In addition, these ligands, except α-(methylenecyclopropyl)glycine, formed H-bond with one of the Ala9 (Figs. 6–10). Interestingly, canavanine formed another H-bond with the nearby Val6 on one of the M2 subunit (Fig. 6). This additional H-bond suggested a more stable canavanine–M2 interaction.

The structural information and the H-bond data suggested that the all Ser10s in the M2 tetramer were critical for ligand binding. This is in agreement with other researches on M2 structures (Du *et al.*, 2010). The distances between a ligand and each of the Ser10 are illustrated in Fig. 11. For amantadine, Ser10 on M2 subunit chain C was brought to closer approximation to the ligand at 46.18 ns during MD simulation (Fig. 12, Video S1). This implies that amantadine is able to hold the M2 subunits close at around 6 Å range under stable docking conformation, and consequently block the ion channel. This result agreed with the inhibitory effect of amantadine. In each selected ligands, the stable molecular poses were approximately 4 Å distance to each of the Ser10, implying their potency in blocking ion channel. In a closer observation, the first three selected compounds, canavanine, α-(methylenecyclopropyl)glycine and quinic acid, maintained stable and close distances to each Ser10. Conversely, 2-hydroxy-3-(3,4-dihydroxyphenyl) and β-D-fructofuranose held only three out of four Ser10s at close approximation. Nevertheless, the short distances between Ser10s and each ligand implied closed ion channel conformation.

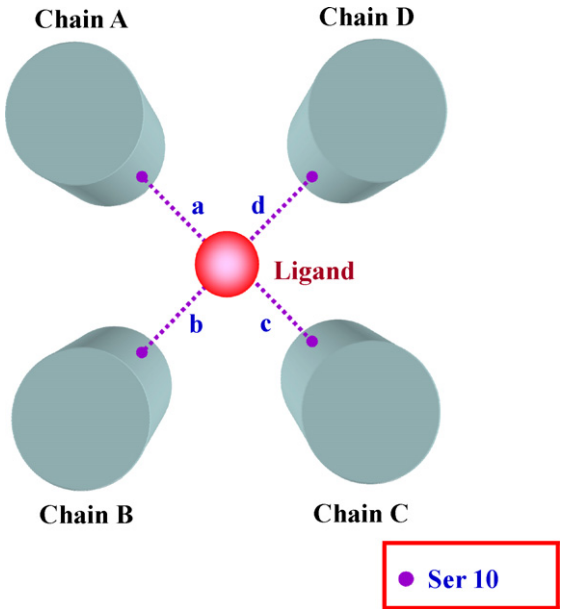

Fig. 11. Schematic diagram for ligand position. The distance between the ligand and Ser 10 in M2 binding site are represented by a–d.

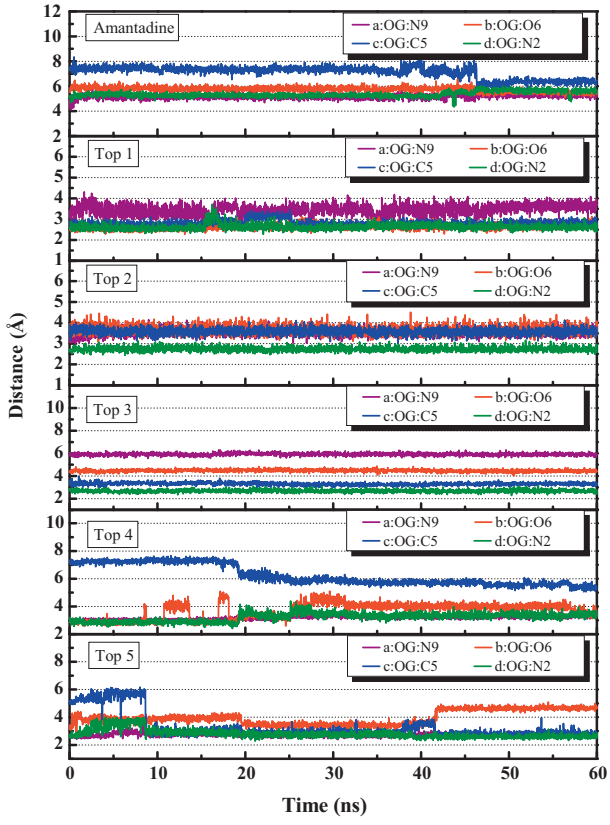

Fig. 12. Time dependence of distance between ligand and Ser 10 during 60 ns simulation.

4. Conclusion

This study investigated the inhibitory potency of a selected set of TCM compounds using MD analysis. The best-fit TCM compounds as well as the control were selected after docking to M2. MD simulation on each selected protein–ligand complex identified Ala9 and Ser10 on each M2 homologous subunit were key residues in stabilizing M2 inhibitors. All five candidate compounds, canavanine, α-(methylenecyclopropyl)glycine, quinic acid, 2-hydroxy-3-(3,4-dihydroxyphenyl)propanoic acid, and β-D-fructofuranose, show stable bindings to the M2 ion channel during simulation. This research implied new potential compounds for influenza treatment. Furthermore, MD analysis on M2–ligand conformations determined the key M2 residues for stabilizing inhibitors. This discovery provides insights to target-specific drug design.

Acknowledgements

The research was supported by grants from the National Science Council of Taiwan (NSC 99-2221-E-039-013), China Medical University (CMU98-TCM, CMU99-S-02, CMU99-TCM) and Asia University (CMU98-ASIA-09). This study is also supported in part by Taiwan Department of Health Clinical Trial and Research Center of Excellence (DOH100-TD-B-111-004) and Taiwan Department of Health Cancer Research Center of Excellence (DOH100-TD-C-111-005). We are grateful to the National Center of High-performance Computing for computer time and facilities.

Appendix A. Supplementary data

Supplementary data associated with this article can be found, in the online version, at doi:10.1016/j.jtice.2011.01.006.

References

Chen, C. Y. C., "TCMDatabase@Taiwan: The World's Largest Traditional Chinese Medicine Database for Drug Screening in Silico," *PLoS ONE*, **6**, e15939 (2011).
Chen, C. Y., "Insights into Designing the Dual-Targeted Her2/Hsp90 Inhibitors," *J. Mol. Graph. Model.*, **29**, 21 (2010a).
Chen, C. Y., "Virtual Screening and Drug Design for Pde-5 Receptor from Traditional Chinese Medicine Database," *J. Biomol. Struct. Dyn.*, **27**, 627 (2010b).
Chen, C. Y. C., "Bioinformatics, Chemoinformatics, and Pharmainformatics Analysis of Her2/Hsp90 Dual-Targeted Inhibitors," *J. Taiwan Inst. Chem. Engrs.*, **41**, 143 (2010c).
Chen, C. Y. C., "Chemoinformatics and Pharmacoinformatics Approach for Exploring the Gaba-a Agonist from Chinese Herb Suanzaoren," *J. Taiwan Inst. Chem. Engrs.*, **40**, 36 (2009a).
Chen, C. Y. C., "Computational Screening and Design of Traditional Chinese Medicine (Tcm) to Block Phosphodiesterase-5," *J. Mol. Graph. Model.*, **28**, 261 (2009b).
Chen, C. Y. C., "De Novo Design of Novel Selective Cox-2 Inhibitors: From Virtual Screening to Pharmacophore Analysis," *J. Taiwan Inst. Chem. Engrs.*, **40**, 55 (2009c).
Chen, C. Y. C., "Pharmacoinformatics Approach for Mpges-1 in Anti-Inflammation by 3d-Qsar Pharmacophore Mapping," *J. Taiwan Inst. Chem. Engrs.*, **40**, 155 (2009d).
Chen, C. Y. C., "Weighted Equation and Rules – A Novel Concept for Evaluating Protein–Ligand Interaction," *J. Biomol. Struct. Dyn.*, **27**, 271 (2009e).
Chen, C. Y. C., "Discovery of Novel Inhibitors for C-Met by Virtual Screening and Pharmacophore Analysis," *J. Chin. Inst. Chem. Engrs.*, **39**, 617 (2008a).
Chen, C. Y. C., "Insights into the Suanzaoren Mechanism-from Constructing the 3d Structure of Gaba-a Receptor to Its Binding Interaction Analysis," *J. Chin. Inst. Chem. Engrs.*, **39**, 663 (2008b).
Chen, C. Y. C., "A Novel Perspective on Designing the Inhibitor of Her2 Receptor," *J. Chin. Inst. Chem. Engrs.*, **39**, 291 (2008c).
Chen, Y. C., "The Molecular Dynamic Simulation of Zolpidem Interaction with Gamma Aminobutyric Acid Type a Receptor," *J. Chin. Chem. Soc.*, **54**, 653 (2007).
Chen, Y. C. and K. T. Chen, "Novel Selective Inhibitors of Hydroxyxanthone Derivatives for Human Cyclooxygenase-2," *Acta Pharmacol. Sin.*, **28**, 2027 (2007).
Chen, C. Y., H. J. Huang, F. J. Tsai, and C. Y. C. Chen, "Drug Design for Influenza a Virus Subtype H1n1," *J. Taiwan Inst. Chem. Engrs.*, **41**, 8 (2010).
Chen, C. Y., Y. H. Chang, D. T. Bau, H. J. Huang, F. J. Tsai, C. H. Tsai, and C. Y. C. Chen, "Discovery of Potent Inhibitors for Phosphodiesterase 5 by Virtual Screening and Pharmacophore Analysis," *Acta Pharmacol. Sin.*, **30**, 1186 (2009).
Chen, C. Y., Y. H. Chang, D. T. Bau, H. J. Huang, F. J. Tsai, C. H. Tsai, and C. Y. C. Chen, "Ligand-Based Dual Target Drug Design for H1n1: Swine Flu – A Preliminary First Study," *J. Biomol. Struct. Dyn.*, **27**, 171 (2009).
Chen, C. Y. C., G. W. Chen, and W. Y. C. Chen, "Molecular Simulation of Her2/Neu Degradation by Inhibiting Hsp90," *J. Chin. Chem. Soc.*, **55**, 297 (2008).
Chen, C. Y. C., Y. F. Chen, C. H. Wu, and H. Y. Tsai, "What Is the Effective Component in Suanzaoren Decoction for Curing Insomnia? Discovery by Virtual Screening and Molecular Dynamic Simulation. *J. Biomol. Struct. Dyn.*, **26**, 57 (2008).

Cheng, P. K., T. W. Leung, E. C. Ho, P. C. Leung, A. Y. Ng, M. Y. Lai, and W. W. Lim, "Oseltamivir- and Amantadine-Resistant Influenza Viruses a (H1n1)," *Emerging Infect. Dis.*, **15**, 966 (2009).

Du, Q. S., R. B. Huang, S. Q. Wang, and K. C. Chou, "Designing Inhibitors of M2 Proton Channel against H1n1 Swine Influenza Virus," *Plos One*, **5**, e9388 (2010).

Helenius, A., "Unpacking the Incoming Influenza Virus," *Cell*, **69**, 577 (1992).

Hsieh, Y. H., F. H. Chu, Y. S. Wang, S. C. Chien, S. T. Chang, J. F. Shaw, C. Y. Chen, W. W. Hsiao, Y. H. Kuo, and S. Y. Wang, "Antrocamphin a, an Anti-Inflammatory Principal from the Fruiting Body of Taiwanofungus Camphoratus, and Its Mechanisms," *J. Agric. Food Chem.*, **58**, 3153 (2010).

Huang, H. J., C. Y. Chen, H. Y. Chen, F. J. Tsai, and C. Y. C. Chen, "Computational Screening and Qsar Analysis for Design of Amp-Activated Protein Kinase Agonist," *J. Taiwan Inst. Chem. Engrs.*, **41**, 352 (2010).

Huang, H. J., K. J. Lee, H. W. Yu, C. Y. Chen, C. H. Hsu, H. Y. Chen, F. J. Tsai, and C. Y. C. Chen, "Structure-Based and Ligand-Based Drug Design for Her 2 Receptor," *J. Biomol. Struct. Dyn.*, **28**, 23 (2010).

Huang, H. J., K. J. Lee, H. W. Yu, H. Y. Chen, F. J. Tsai, and C. Y. Chen, "A Novel Strategy for Designing the Selective Ppar Agonist by The "Sum of Activity" Model," *J. Biomol. Struct. Dyn.*, **28**, 187 (2010).

Ilyushina, N. A., E. A. Govorkova, and R. G. Webster, "Detection of Amantadine-Resistant Variants among Avian Influenza Viruses Isolated in North America and Asia," *Virology*, **341**, 102 (2005).

Lipinski, C. A., F. Lombardo, B. W. Dominy, and P. J. Feeney, "Experimental and Computational Approaches to Estimate Solubility and Permeability in Drug Discovery and Development Settings," *Adv. Drug Deliv. Rev.*, **46**, 3 (2001).

Patil, R., S. Das, A. Stanley, L. Yadav, A. Sudhakar, and A. K. Varma, "Optimized Hydrophobic Interactions and Hydrogen Bonding at the Target–Ligand Interface Leads the Pathways of Drug-Designing," *Plos One*, **5** (2010).

Pinto, L. H., G. R. Dieckmann, C. S. Gandhi, C. G. Papworth, J. Braman, M. A. Shaughnessy, J. D. Lear, R. A. Lamb, and W. F. DeGrado, "A Functionally Defined Model for the M2 Proton Channel of Influenza a Virus Suggests a Mechanism for Its Ion Selectivity," *Proc. Natl. Acad. Sci. U.S.A.*, **94**, 11301 (1997).

Pinto, L. H. and R. A. Lamb, "The M2 Proton Channels of Influenza a and B Viruses," *J. Biol. Chem.*, **281**, 8997 (2006).

Squires, B., C. Macken, A. Garcia-Sastre, S. Godbole, J. Noronha, V. Hunt, R. Chang, C. N. Larsen, E. Klem, K. Biersack, and R. H. Scheuermann, "Biohealthbase: Informatics Support in the Elucidation of Influenza Virus Host Pathogen Interactions and Virulence," *Nucleic Acids Res.*, **36**, D497 (2008).

Stouffer, A. L., R. Acharya, D. Salom, A. S. Levine, L. Di Costanzo, C. S. Soto, V. Tereshko, V. Nanda, S. Stayrook, and W. F. DeGrado, "Structural Basis for the Function and Inhibition of an Influenza Virus Proton Channel," *Nature*, **451**, 596 (2008).

Su, C. R., Y. F. Chen, M. J. Liou, H. Y. Tsai, W. S. Chang, and T. S. Wu, "Anti-Inflammatory Activities of Furanoditerpenoids and Other Constituents from Fibraurea Tinctoria," *Bioorg. Med. Chem.*, **16**, 9603 (2008).

Sugrue, R. J. and A. J. Hay, "Structural Characteristics of the M2 Protein of Influenza a Viruses: Evidence That It Forms a Tetrameric Channel," *Virology*, **180**, 617 (1991).

Tang, Y. J., J. S. Yang, C. F. Lin, W. C. Shyu, M. Tsuzuki, C. C. Lu, Y. F. Chen, and K. C. Lai, "Houttuynia Cordata Thunb Extract Induces Apoptosis through Mitochondrial-Dependent Pathway in Ht-29 Human Colon Adenocarcinoma Cells," *Oncol. Rep.*, **22**, 1051 (2009).

Venkatachalam, C. M., X. Jiang, T. Oldfield, and M. Waldman, "Ligandfit: A Novel Method for the Shape-Directed Rapid Docking of Ligands to Protein Active Sites," *J. Mol. Graph. Model.*, **21**, 289 (2003).